The Anti-Amyloidogenic Effect Is Exerted against Alzheimer's β-Amyloid Fibrils in Vitro by Preferential and Reversible Binding of Flavonoids to the Amyloid Fibril Structure†

Mie Hirohata,[‡,§,||] Kazuhiro Hasegawa,[‡,§] Shinobu Tsutsumi-Yasuhara,[‡] Yumiko Ohhashi,[‡] Tadakazu Ookoshi,[‡] Kenjiro Ono,[||] Masahito Yamada,[||] and Hironobu Naiki*[,‡,⊥]

Division of Molecular Pathology, Department of Pathological Sciences, Faculty of Medical Sciences, University of Fukui, Fukui 910-1193, Japan, Department of Neurology and Neurobiology of Aging, Kanazawa University Graduate School of Medical Science, Kanazawa 920-8640, Japan, and CREST, Japan Science and Technology Agency, Saitama 332-0012, Japan

Received July 31, 2006; Revised Manuscript Received December 13, 2006

ABSTRACT: How various anti-amyloidogenic compounds inhibit the formation of Alzheimer's β-amyloid fibrils (fAβ) from amyloid β-peptide (Aβ) and destabilize fAβ remains poorly understood. Using spectrophotometry, spectrofluorometry, atomic force microscopy, sodium dodecyl sulfate−polyacrylamide gel electrophoresis, and surface plasmon resonance (SPR), we investigated the anti-amyloidogenic effects of five flavonoids on fAβ in vitro. Oxidized flavonoids generally inhibited fAβ(1−40) formation significantly more potently than fresh compounds. Characterization of the novel fluorescence of myricetin (Myr) emitted at 575 nm with an excitation maximum at 430 nm in the presence of fAβ(1−40) revealed the specific binding of Myr to fAβ(1−40). By SPR analysis, distinct association and dissociation reactions of Myr with fAβ(1−40) were observed, in contrast to the very weak binding to the Aβ monomer. A significant decrease in the rate of fibril extension was observed when >0.5 μM Myr was injected into the SPR experimental system. These findings suggest that flavonoids, especially Myr, exert an anti-amyloidogenic effect in vitro by preferentially and reversibly binding to the amyloid fibril structure of fAβ, rather than to Aβ monomers.

Alzheimer's disease (AD)[1] is characterized by the abundance of intraneuronal neurofibrillary tangles and the extracellular deposition of the amyloid β-peptide (Aβ) as amyloid plaques and vascular amyloid (*1*). On the basis of compelling genetic evidence, pathological assemblies of Aβ are said to be the cause of all forms of AD (*2*). Despite recent progress in the symptomatic therapy with cholinergic drugs (*3*), an effective therapeutic approach that interferes directly with the neurodegenerative process in AD, especially the accumulation of Aβ in the central nervous system, remains to be developed. Recently, immunization with Aβ (*4*) and treatment with a copper zinc chelator (*5*) were reported to attenuate the accumulation of Aβ in AD transgenic mice.

A nucleation-dependent polymerization model has been proposed to explain the general mechanism of amyloid fibril formation in vitro (*6*−*9*). This model consists of two phases, i.e., nucleation and extension phases. Nucleus formation requires a series of association steps of monomers, which are thermodynamically unfavorable, representing the rate-limiting step in amyloid fibril formation in vitro. Once the nucleus (*n*-mer) has been formed, the next step becomes thermodynamically favorable, resulting in rapid extension of amyloid fibrils with further addition of monomers to the nucleus in accordance with a first-order kinetic model, i.e., via the consecutive association of precursor proteins onto the ends of existing fibrils (*9*).

On the basis of this model and by using fluorescence spectroscopy with thioflavin T (ThT) and electron microscopy (EM), we systematically demonstrated that several classes of organic compounds not only inhibit the formation of β-amyloid fibrils (fAβ) from Aβ and their extension but also destabilize fAβ dose-dependently in vitro. These compounds included nordihydroguaiaretic acid (*10*, *11*), curcumin

† This research was supported in part by Grants-in-Aid for Scientific Research on Priority Areas (Life of Proteins and Water & Biomolecules) from the Ministry of Education, Culture, Sports, Science and Technology, Japan (H.N.), for Research on Specific Diseases from Ministry of Health, Labour and Welfare, Japan (H.N.), and for 21st Century COE program "Biomedical Imaging Technology Integration Program" from the Japan Society of the Promotion of Science (JSPS) (H.N.).

* To whom correspondence should be addressed: Division of Molecular Pathology, Department of Pathological Sciences, Faculty of Medical Sciences, University of Fukui, Fukui 910-1193, Japan. Telephone: +81-776-61-8320. Fax: +81-776-61-8123. E-mail: naiki@fmsrsa.fukui-med.ac.jp.

‡ University of Fukui.

§ These authors contributed equally to this work.

|| Kanazawa University Graduate School of Medical Science.

⊥ CREST, Japan Science and Technology Agency.

[1] Abbreviations: Aβ, amyloid β-peptide; AD, Alzheimer's disease; AFM, atomic force microscopy; α-syn, α-synuclein; BSA, bovine serum albumin; Cat, (+)-catechin; Cys-Aβ(1−40), N-terminally Cys-containing Aβ(1−40); DMSO, dimethyl sulfoxide; EDC, *N*-ethyl *N*′-[3-(dimethylamino)propyl]carbodiimide hydrochloride; EDTA, ethylenediaminetetraacetic acid; EM, electron microscopy; epi-Cat, (−)-epicatechin; fAβ, β-amyloid fibrils; Gdn-HCl, guanidine hydrochloride; Mor, morin; Myr, myricetin; NaOAc, sodium acetate; NHS, *N*-hydroxysuccinimide; NMR, nuclear magnetic resonance; PB_{sol}, phosphate buffer-soluble; Qur, quercetin; RU, response unit; SDS_{Insol}, sodium dodecyl sulfate-insoluble; SDS−PAGE, SDS−polyacrylamide gel electrophoresis; SDS_{sol}, SDS-soluble; SPR, surface plasmon resonance; ThT, thioflavin T.

10.1021/bi061540x CCC: $37.00
Published on Web 01/25/2007

and rosmarinic acid (*12*), wine-related polyphenols [myricetin (Myr), quercetin (Qur), morin (Mor), kaempferol, (+)-catechin (Cat), and (−)-epicatechin (epi-Cat)] (*13*), tannic acid (*14*), vitamin A (retinol, retinal, and retinoic acid) and *β*-carotene (*15*), rifampicin and tetracycline (*10*, *11*, *14*), nicotine (*16*), coenzyme Q10 (*17*), nonsteroidal anti-inflammatory drugs (*18*), and anti-Parkinsonian agents (dopamine, selegiline, L-dopa, pergolide, and bromocriptine) (*19*). We found significant positive correlations of the effective concentrations (EC_{50}) of these compounds ranging from 10 nM to 10 μM, for the formation and destabilization of fA*β*-(1−40) and fA*β*(1−42) (*19*). Other groups also reported the anti-amyloidogenic and fibril-destabilizing activity of various compounds and peptides for fA*β*s, including rifampicin (*20*, *21*), small-molecule anionic sulfonates or sulfates (*22*), *β*-sheet breaker peptides (*23*), melatonin (*24*), tetracyclines (*25*), and nicotine (*26*). Recently, Taniguchi et al. tested 42 compounds that belong to nine different chemical classes for their ability to inhibit heparin-induced assembly of tau into filaments, as well as fA*β* formation in vitro (*27*).

Many anti-amyloidogenic compounds have been reported, but how they inhibit fA*β* formation from A*β* and destabilize fA*β* remains poorly understood. By using circular dichroism, EM, and nuclear magnetic resonance (NMR) spectroscopy, Pappolla et al. studied the interaction of melatonin with A*β*-(1−40) and A*β*(1−42) (*24*). On the basis of NMR spectroscopic studies, Zeng et al. observed that nicotine shows only modest binding to A*β*(1−42) in a predominantly α-helical or random, extended chain structure, indicating that the inhibition of fA*β* formation by nicotine probably results from binding to a small, soluble *β*-sheet aggregate that is NMR invisible (*26*). On the other hand, using electron spin resonance spectrometric analysis, Tomiyama et al. (*21*) found that at least one mechanism of rifampicin-mediated inhibition of A*β* aggregation and neurotoxicity involves scavenging of free radicals.

In this paper, we report the molecular mechanisms underlying the anti-amyloidogenic effects of five flavonoids (Figure 1) determined by spectrophotometric and spectrofluorometric analysis, atomic force microscopic examination, sodium dodecyl sulfate−polyacrylamide gel electrophoresis (SDS−PAGE), and surface plasmon resonance (SPR) analysis of fA*β* in vitro. We found evidence that these compounds, especially Myr, exert their anti-amyloidogenic effect in vitro by preferentially and reversibly binding to the amyloid fibril structure of fA*β*, rather than to A*β* monomers.

EXPERIMENTAL PROCEDURES

UV−Vis Spectroscopy of Flavonoids

The reaction mixture contained 25 μM flavonoids (Myr, Qur, Mor, Cat, or epi-Cat, Sigma Chemical Co., St. Louis, MO), 1% dimethyl sulfoxide (DMSO) (Nacakai Tesque, Inc., Kyoto, Japan), 50 mM phosphate buffer (pH 7.5), and 100 mM NaCl. The mixture (500 μL) was put into a semi-micro quartz cell (10 mm light path, 2 mm inner width), capped and sealed with Parafilm, and then incubated at 37 °C. The time-dependent changes in UV−vis spectra (250−600 nm) were recorded using a Beckman DU-640 spectrophotometer with a scan speed of 120 nm/min at 37 °C.

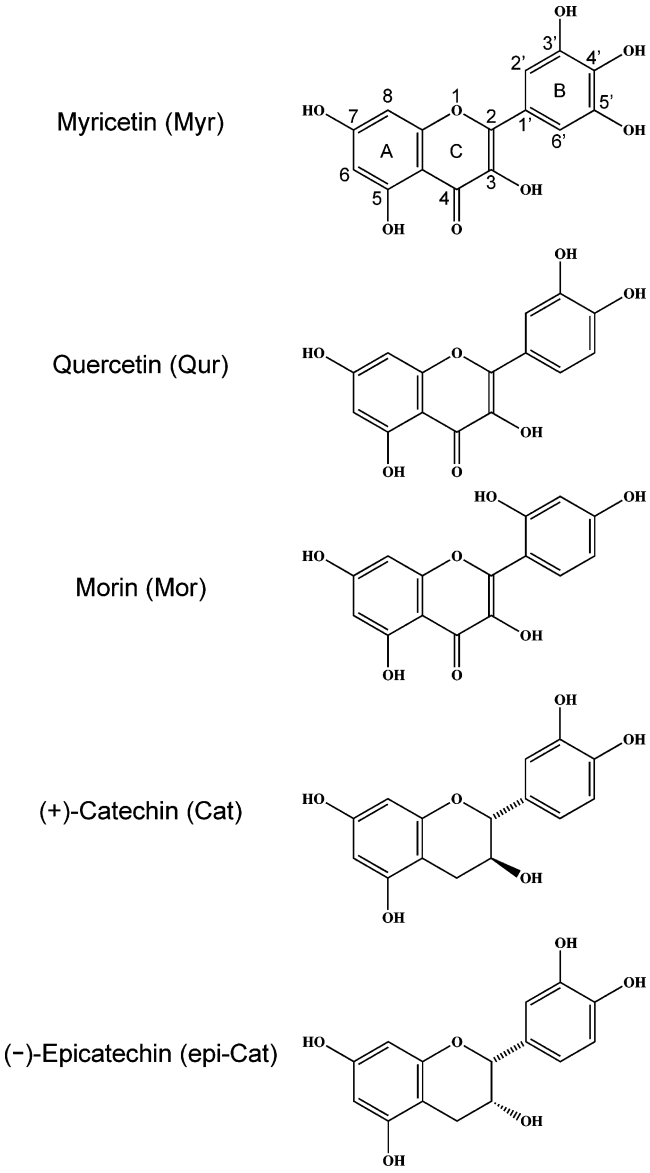

FIGURE 1: Structures of flavonoids examined in this study.

*Preparation of A*β *and fA*β *Solutions*

A*β*(1−40) (trifluoroacetate salt, lot numbers 530108, 541226, and 550927, Peptide Institute Inc., Osaka, Japan) was dissolved by being briefly vortexed in a 0.02% ammonia solution at a concentration of 500 μM (2.2 mg/mL) in a 4 °C room and stored at −80 °C before being assayed [fresh A*β*(1−40) solutions]. Protein concentrations of A*β* and fA*β* in the reaction mixtures were determined by the method of Bradford (*28*) with a protein assay kit (Bio-Rad Laboratories, Inc., Hercules, CA). The A*β*(1−40) solution quantified by amino acid analysis was used as the standard. fA*β*(1−40) were formed from the fresh A*β*(1−40) solutions, sonicated, and stored at 4 °C as described elsewhere (*29*).

To obtain fA*β*(1−40) that were not clumped together, sonicated fA*β*(1−40) were extended with fresh A*β*(1−40) solutions, just before the destabilization reaction (*11*, *16*). The reaction mixture volume was 300 μL and contained 10 μg/mL (2.3 μM) fA*β*(1−40), 50 or 100 μM A*β*(1−40), 50 mM phosphate buffer (pH 7.5), and 100 mM NaCl. After incubation at 37 °C for 3−6 h under nonagitated conditions, the extension reaction proceeded to equilibrium as measured

by the fluorescence of ThT. In the following experiment, the concentration of fAβ(1−40) in the final reaction mixture was regarded as 50 or 100 μM.

fAβ Polymerization Assay with Flavonoids

Polymerization of Aβ with or without fAβ added as seeds was assayed as described elsewhere (*10*). The reaction mixture contained 50 μM Aβ(1−40), 0 or 10 μg/mL fAβ-(1−40), 0, 25, or 50 μM flavonoids (Myr, Qur, Mor, Cat, and epi-Cat), 1% DMSO, 50 mM phosphate buffer (pH 7.5), and 100 mM NaCl. Flavonoids dissolved in DMSO at concentrations of 2.5 and 5 mM were added to the reaction mixture to make the final concentrations 25 and 50 μM, respectively.

In some experiments, flavonoids were oxidized prior to the incubation. Briefly, prior to the addition of Aβ(1−40) and fAβ(1−40), the reaction mixtures were preincubated at 37 °C for 24 h just as described below. Aβ(1−40) and fAβ-(1−40) were added to the reaction mixture which was then incubated for various durations.

Aliquots (30 μL) of the mixture were put into oil-free PCR tubes (size, 0.5 mL; code number, 9046; Takara Shuzo Co. Ltd., Otsu, Japan). The reaction tubes were sealed in a chamber saturated with water vapor, put into an air incubator (MIR-153, Sanyo Electric Co. Ltd., Osaka, Japan), and incubated at 37 °C. Incubation times ranged between 0 and 7 days, and the reaction was stopped by placing the tubes on ice. The reaction tubes were not agitated during the reaction. Triplicate 5 μL aliquots from each reaction tube were subjected to fluorescence spectroscopy, and the mean of each triplicate was determined. In the ThT solution, the concentration of flavonoids examined in this study was diluted up to 1/200 of that in the reaction mixture. We confirmed that these compounds did not quench ThT fluorescence at the diluted concentration (data not shown).

fAβ Destabilization Assay with Flavonoids

Destabilization of fAβ was assayed as described elsewhere (*11*). Briefly, the reaction mixture contained 25 μM fAβ-(1−40), 0, 25, or 50 μM flavonoids, 1% DMSO, 50 mM phosphate buffer (pH 7.5), and 100 mM NaCl. In some experiments, flavonoids were oxidized prior to the incubation vide supra. After being mixed by pipetting, triplicate 5 μL aliquots were subjected to fluorescence spectroscopy, and 30 μL aliquots were put into oil-free PCR tubes (Takara Shuzo Co. Ltd.). The reaction tubes were sealed in a chamber saturated with water vapor, put into an air incubator, and incubated at 37 °C. Incubation times ranged from 0 to 24 h, and the reaction was stopped by placing the tubes on ice. The reaction tubes were not agitated during the reaction. From each reaction tube, 5 μL aliquots in triplicate were subjected to fluorescence spectroscopy, and the mean of the three measurements was determined. ThT fluorescence did not change significantly when fAβ were incubated with 0−50 μM flavonoids at either 4 or 37 °C for 1 min and then subjected to a ThT assay, indicating that these compounds did not compete with ThT for fAβ (data not shown).

Fluorescence Spectroscopy

fAβ(1−40) was quantitated using ThT as described by Naiki and Nakakuki (*30*) on a Hitachi (Tokyo, Japan) F-4500 fluorescence spectrophotometer. The optimal fluorescence of fAβ(1−40) was measured at the excitation and emission wavelengths of 445 and 490 nm, respectively, with the reaction mixture (1 mL) containing 5 μM ThT (Wako Pure Chemical Industries Ltd., Osaka, Japan) and 50 mM glycine-NaOH buffer (pH 8.5).

The novel fluorescence emission of Myr bound to fAβ-(1−40) was characterized as follows. The reaction mixtures (200 μL) containing 0−50 μM Myr, 50 mM buffer, 100 mM NaCl, and 0−50 μM fAβ(1−40), or 25 μM monomeric Aβ-(1−40), were analyzed at 25 °C with a black microfluorimeter cell (GL Sciences Inc., Tokyo, Japan). The buffers used were citrate buffer at pH 4−6, phosphate buffer at pH 6−8, Tris-HCl buffer at pH 8−9, and glycine-NaOH buffer at pH 8.5−10. The actual pH of each reaction mixture was measured with a compact pH meter (B-212, Horiba, Ltd., Kyoto, Japan). Excitation and emission fluorescence spectra were obtained immediately after the reaction mixture was made. Excitation and emission were scanned in the range of 320−550 nm (emission at 575 nm) and 450−600 nm (excitation at 430 nm), respectively. The scanning speed was 240 nm/min, and excitation and emission slits were set at 5 and 5 nm, respectively. Every scanning was finished in 4 min, and the peak fluorescence intensities (excitation at 430 nm and emission at 575 nm) were recorded. We confirmed that the peak fluorescence of Myr (excitation at 430 nm and emission at 575 nm) did not change for at least 5 min after the reaction mixture was made (data not shown).

Atomic Force Microscopy (AFM)

AFM was carried out in air using an SPA-400 scanning probe microscope controlled by an SPI 3800F probe station (Seiko Instruments Inc., Tokyo, Japan). The cantilevers that were used (SI-DF20AL, Seiko Instruments Inc.) were rectangular and had a force contact of 12 N/m and a resonance frequency of 128 kHz at tip scan rates from 0.5 to 1 Hz. Ten microliters of the reaction mixture was spotted onto freshly cleaved mica (Okenshoji Co. Ltd., Tokyo, Japan), incubated for 2 min at room temperature to allow fAβs to adhere to the surface, and then washed briefly with water to reduce the background contaminants. All images were collected as the variable deflection images in a dynamic force mode in air at room temperature, containing height, phase, and error channel data. At least four regions of the mica surface were examined to confirm the homogeneity of the structures throughout the sample. Section analysis was accomplished by drawing a line over the individual globular species and measuring the distance from the mica surface to the top of the structure. This was done four times, and an average was obtained.

Fractionation of the Reaction Mixture, SDS−PAGE, and Densitometry

Aβ(1−40) in the reaction mixtures of fAβ(1−40) polymerization, extension, and destabilization were fractionated into phosphate buffer-soluble (PB_{sol}), SDS-soluble (SDS_{sol}), and SDS-insoluble (SDS_{Insol}) fractions and then subjected to SDS−PAGE, as follows. Aliquots (30 μL) of the reaction mixtures were removed and centrifuged at 21500*g* for 1 h at 4 °C. After removal of the supernatants containing Aβ-(1−40) soluble in phosphate buffer (PB_{sol} fraction), 30 μL

of 50 mM Tris-HCl (pH 7.5) containing 4% SDS was added to the pellets, vortex-mixed, incubated at room temperature for 20 min, and then centrifuged at 21500*g* for 1 h at 4 °C. After removal of the supernatants containing Aβ(1−40) soluble in 4% SDS (SDS_{sol} fraction), the supernatants and the pellets were independently dried in a centrifugation evaporator for 2 h at 37 °C. Then, 30 μL of 73% formic acid was added to the pellets containing Aβ(1−40) insoluble in 4% SDS (SDS_{Insol} fraction), vortex-mixed, incubated at room temperature for 1 h, and dried in a centrifugation evaporator for 2 h at 37 °C. The PB_{sol} fraction was dried in a centrifugation evaporator for 1 h at 37 °C. Twenty microliters of SDS sample buffer was added to these dried fractions and then subjected to SDS−PAGE (15% acrylamide, at 60 V for 3 h) as described by Schägger and von Jagow (*31*).

After Coomassie Brilliant Blue staining, the density of the monomeric Aβ(1−40) band in each fraction was quantified by scanning densitometry, using the FluorChem IS-8000 Advanced Fluorescence, Chemiluminescence and Visible Light Imaging System (Alpha Innotech Corp., San Leandro, CA) with AlphaEaseFC image processing and analysis software.

Affinity Analysis of Flavonoids to Aβ/fAβ by SPR

Immobilization of Aβ/fAβ on the Sensor Chip of a Biacore Biosensor. fAβ stored at 4 °C were centrifuged at 4 °C for 2 h at 16000*g*. fAβ had precipitated completely as measured by the fluorescence of ThT. The pellet was resuspended in water, sonicated, diluted with 10 mM sodium acetate (NaOAc) (pH 4.0), and then immobilized immediately on the CM5 sensor chip (Biacore AB, Uppsala, Sweden) by amine coupling. The carboxymethyl dextran surface was activated by 70 μL of a mixture of 0.4 M *N*-ethyl-*N*′-[3-(dimethylamino)propyl]carbodiimide hydrochloride (EDC) and 0.1 M *N*-hydroxysuccinimide (NHS), at an injection rate of 5 μL/min. After immobilization of fAβ, the remaining activated groups were blocked with 70 μL of 1 M ethanolamine (pH 9.0). The reference cell was prepared by the above-described amine coupling without addition of fAβ. The final responses of the immobilized fAβ were 7700−8060 response units (RU).

N-Terminally Cys-containing Aβ(1−40) [Cys-Aβ(1−40)] (code 16509, Anaspec Inc., San Jose, CA) was immobilized on the surface of a sensor chip by the methods of Cairo et al. (*32*) with some modification. The surface of the CM5 sensor chip was activated by EDC/NHS as described above, and then 70 μL of 1 M ethylenediamine (pH 8.5) was injected to introduce amine residue. Subsequently, *N*-(8-maleimidocapryloxy)sulfosuccinimide was injected to generate a surface modified with maleimide residue. Cys-Aβ(1−40) was dissolved in 10% DMSO and stored at −80 °C. The stock solution was diluted with 10 mM NaOAc (pH 5.0) to yield the final concentration of 16 μM and injected onto the maleimide-activated surface. The remaining activated groups were blocked by 70 μL of 100 mM cysteine and 10 mM NaOAc (pH 5.0). Noncovalently attached peptide or aggregated Cys-Aβ(1−40) was removed by the injection of 6 M guanidine hydrochloride (Gdn-HCl) (pH 7.5). The final responses of the immobilized peptide were 3800−4300 RU. The reference cell was prepared by the above-described coupling without addition of Cys-Aβ(1−40).

The affinity of Mor for Aβ(1−40) was analyzed by immobilizing Aβ(1−40) by NHS/EDC coupling (700 RU) just in the same way as in the case of fAβ vide supra, since Mor significantly bound to a Cys-immobilized blank flow cell.

Affinity Analysis. The SPR experiments were performed with a Biacore 3000 device (Biacore AB). The reaction was performed at 37 °C unless otherwise noted, using the running buffer [50 mM phosphate (pH 7.5), 100 mM NaCl, 3 mM ethylenediaminetetraacetic acid (EDTA), 0.005% Tween 20, and 1% DMSO]. Flavonoids dissolved in DMSO were added to the running buffer to make the final concentration 0−25 μM and then injected over the reference and Aβ/fAβ-immobilized flow cells at a flow rate of 30 μL/min. Each cycle consisted of a waiting phase (10 or 15 min), an injection phase of flavonoids (8 min), a dissociation phase of flavonoids (12 min), and a regeneration phase of sensor surface. The surface of the sensor chip immobilized with Aβ peptide was regenerated with sequential injections of 6 M Gdn-HCl, 0.1% SDS, and 1.5 M Gly-HCl (pH 2.5). The surface with fAβ was regenerated with 0.1% SDS. The sensorgrams were compensated using "double referencing" (*33*). Solvent effects were further compensated by a DMSO calibration procedure (*34*), with calibration solutions ranging from 0.4 to 1.9% DMSO.

Analysis of the Effect of Myr on the fAβ Extension Using SPR

The CM3 sensor chip was used for the analysis of fAβ extension as described previously (*33*). The seed fAβ was prepared from Aβ(1−40) (trifluoroacetate salt, bulk type, lot no. 530927, Peptide Institute Inc.) and immobilized on the surface of flow cells 2 and 4 (512−600 RU). Blank cells 1 and 3 were prepared as described above. The pairs of flow cells 2 and 1 and flow cells 4 and 3 were used for control and Myr-interference extension analysis, respectively. These two types of analysis were performed in parallel at Myr concentrations of 0, 0.2, 0.5, 1, 2, 5, 10, and 25 μM. For the positive control reaction, 100 μL of running buffer was first injected into flow cells 2 and 1, followed by the injection of a 5 μM Aβ solution (30 μL) using COINJECT mode (Figure 9A). For the Myr-interference extension reaction, a 0−25 μM Myr solution (100 μL) was first injected instead of a buffer solution into flow cells 4 and 3, followed immediately by the injection of a 5 μM Aβ solution (30 μL) (Figure 9A). Before the Myr concentration was changed, 100 μL of running buffer was injected into flow cells 2 and 1 and flow cells 4 and 3 in parallel, followed by the injection of a 5 μM Aβ solution (30 μL) to confirm the recovery from Myr interference in flow cells 4 and 3. To offset the intrinsic fluctuation caused by the injection, the sensorgrams were compensated using double referencing (*33*). The data were processed using BIAevaluation version 4.1. The extension rate was calculated as the slope of the linear curve fitting to the extension phase during injection of Aβ solution. Since the observed extension rate decreased cycle by cycle as described previously (*33*), the ratio of inhibition was calculated by dividing the rate of Myr-interference extension by the rate of positive control at the same cycle.

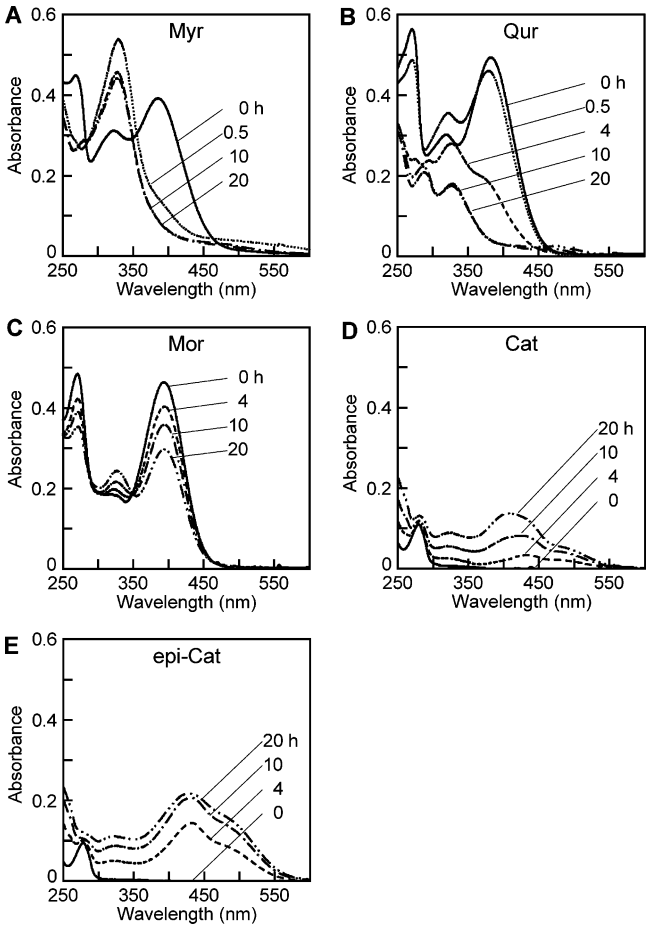

FIGURE 2: Time-dependent changes in the UV−vis spectra of flavonoids. The reaction mixture containing 25 μM flavonoids [Myr (A), Qur (B), Mor (C), Cat (D), and epi-Cat (E)], 1% DMSO, 50 mM phosphate buffer (pH 7.5), and 100 mM NaCl was incubated at 37 °C. Then the UV−vis spectra of the mixture were monitored at 0 (—), 0.5 (•••), 4 (- - -), 10 (•-•), and 20 h (-••-), as described in Experimental Procedures.

Statistical Analysis

The linear least-squares fit, an unpaired *t*-test, and one-way analysis of variance, post-hoc test by Scheffe or Dunnett, were used for statistical analysis.

RESULTS

Time-Dependent Changes in the UV−Vis Spectra of Flavonoids. Flavonols (Myr, Qur, and Mor) exhibited three major characteristic peaks on UV−vis spectroscopy (Figure 2A−C). Band I (382−394 nm) and band II (267−271 nm) are considered to be associated with absorption due to the cinnamoyl system (consisting of the B ring, a double bond between atoms 2 and 3, and 4-keto group of the C ring) and benzoyl system (consisting of the A ring and the 4-keto group of the C ring), respectively (Figure 1) (*35*). The magnitude of the peak at around 320−327 nm that increased with the decrease in the magnitudes of bands I and II may be considered to be associated with the formation of the water adduct to positions 2 and 3 of the C ring during autoxidation (*36*). Each flavonol exhibited characteristic time-dependent changes in these peaks. As shown in Figure 2A, the magnitudes of bands I and II of Myr decreased rapidly with the increase in the magnitude of the peak at around 320−327 nm. The latter peak was stable after incubation for 10 h, suggesting the formation of stable autoxidative intermediate of Myr. The magnitudes of bands I and II of Qur also decreased rapidly along with the transient increase in the magnitude of the peak at around 320−327 nm (Figure 2B). In contrast to the case of Myr, the magnitude of the latter peak decreased after incubation for 0.5 h, suggesting the formation of an unstable autoxidative intermediate of Qur. As shown in Figure 2C, the magnitudes of bands I and II of Mor decreased slowly along with the small increase in the magnitude of the peak at around 320−327 nm.

Flavan-3-ols (Cat and epi-Cat) exhibited a stable peak at 278 nm along with the increase in the magnitudes of the broad peaks at around 350−550 nm during incubation (Figure 2D,E). Although the latter peaks may indicate the formation of procyanidin polymer (condensed tannin) or other oxidative products, we could not identify the details of the product, due to the complex nature of the condensing polymerization or oxidation of flavan-3-ols (*37*).

Effects of Flavonoids on Formation of fAβ(1−40) from Fresh Aβ(1−40) and Their Extension and Destabilization. Incubation of the polymerization-prone lot of Aβ(1−40) with fresh or oxidized flavonoids at pH 7.5, at 37 °C for 24 h, significantly reduced ThT fluorescence ($p < 0.05$, one-way analysis of variance, post-hoc test by Scheffe, Figure 3A). Importantly, oxidized Qur inhibited fAβ(1−40) formation significantly more potently than fresh Qur (54.6 ± 5.5% vs 30.7 ± 2.9%; $p < 0.05$). Incubation of fresh Aβ(1−40) with fAβ(1−40) with fresh or oxidized flavonoids at pH 7.5, at 37 °C for 6 h, reduced significantly ThT fluorescence ($p < 0.05$, one-way analysis of variance, post-hoc test by Scheffe, Figure 3B). Oxidized Myr, Mor, Cat, and epi-Cat inhibited fAβ(1−40) extension significantly more potently than fresh compounds (38.6 ± 2.1 vs 21.7 ± 0.9%, 62.0 ± 1.3 vs 35.3 ± 0.3%, 73.6 ± 2.1 vs 34.9 ± 2.0%, and 75.6 ± 1.9 vs 57.5 ± 5.6%, respectively; $p < 0.05$). After incubation of fAβ(1−40) with fresh or oxidized Myr and Qur at pH 7.5, at 37 °C for 6 h, ThT fluorescence was reduced significantly as compared with controls ($p < 0.05$, one-way analysis of variance, post-hoc test by Scheffe, Figure 3C). Myr exhibited the most potent destabilizing activity among the flavonoids that were examined. Fresh Qur and Mor destabilized fAβ-(1−40) significantly more potently than oxidized compounds (54.6 ± 8.2 vs 76.3 ± 5.7% and 64.4 ± 1.6 vs 82.2 ± 4.7%, respectively; $p < 0.05$).

After incubation of Aβ(1−40) at pH 7.5, at 37 °C for 7 days, typical amyloid fibrils were observed by AFM (Figure 4A). fAβ(1−40) assumed a nonbranched, helical filament structure approximately 10 nm in height and exhibited a helical periodicity of approximately 220 nm. On the other hand, 50 μM Myr markedly reduced the number and length of fAβ(1−40) that formed (Figure 4B). Small amorphous aggregates were occasionally observed (Figure 4B, inset). When fresh Aβ(1−40) was incubated with fAβ(1−40) at pH 7.5, at 37 °C for 6 h, clear fibril extension was observed with some lateral aggregation (Figure 4C). However, 50 μM Myr completely inhibited the extension of sonicated fAβ-(1−40) (Figure 4D). The short rodlike structures observed in Figure 4D may represent not only unextended seed fibrils but also destabilized amyloid fibrils after the extension reaction. After incubation of fAβ(1−40) with Myr at pH 7.5, at 37 °C for 6 h, small amorphous aggregates (Figure 4E)

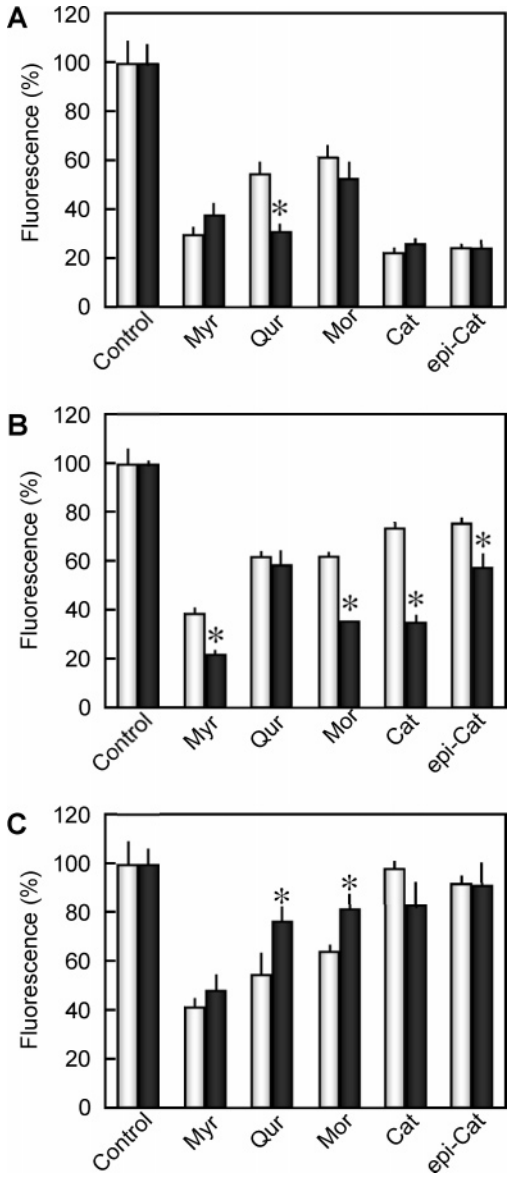

FIGURE 3: Effects of flavonoids on formation of fAβ(1−40) from fresh Aβ(1−40) (A) and their extension (B) and destabilization (C), monitored by ThT fluorescence. In panel A, the reaction mixture containing 50 μM Aβ(1−40) (lot 550927), 50 mM phosphate buffer (pH 7.5), 100 mM NaCl, and 0 or 50 μM fresh (□) or oxidized flavonoids (■) was incubated at 37 °C for 24 h. In panel B, the reaction mixture containing 10 μg/mL (2.3 μM) fAβ(1−40), 50 μM Aβ(1−40), 50 mM phosphate buffer (pH 7.5), 100 mM NaCl, and 0 or 50 μM fresh (□) or oxidized flavonoids (■) was incubated at 37 °C for 6 h. In panel C, the reaction mixture containing 25 μM fAβ(1−40), 50 mM phosphate buffer (pH 7.5), 100 mM NaCl, and 0 or 50 μM fresh (□) or oxidized flavonoids (■) was incubated at 37 °C for 6 h. Each column represents the mean of three independent experiments. The standard deviation is indicated by the bars. Results are given as the percent fluorescence of controls (taken to be 100%). The asterisks denote a p of <0.05, fresh vs oxidized flavonoids, with an unpaired t-test.

as well as short sheared fibrils (Figure 4F) were occasionally observed.

Figure 5 shows the effects of flavonoids on formation of fAβ(1−40) from fresh Aβ(1−40) and their extension and destabilization, determined by SDS−PAGE after fractionation into PB_{sol}, SDS_{sol}, and SDS_{Insol} fractions. Incubation of a polymerization-prone lot of Aβ(1−40) with Myr at pH 7.5, at 37 °C for 24 h, significantly reduced the relative density of the SDS_{Insol} fraction (Figure 5D; 57.7 ± 7.5 vs 93.5 ± 7.5%; $p < 0.05$). On the other hand, Myr significantly increased the relative density of the PB_{sol} and SDS_{sol} fractions (Figure 5D; 17.9 ± 5.2 vs 0.5 ± 1.0% and 24.4 ± 5.7 vs 6.0 ± 7.0%, respectively; $p < 0.05$). This suggests that Myr inhibits the polymerization of Aβ(1−40) by binding to Aβ(1−40) and trapping it in monomeric and SDS-soluble oligomeric states. Alternatively, Myr may bind to fAβ(1−40) and their intermediates, thus inhibiting the addition of Aβ(1−40) onto the growing ends of fAβ(1−40). Myr significantly increased only the relative density of the SDS_{sol} fraction in the extension reaction (Figure 5E; 14.8 ± 3.6 vs 7.0 ± 2.5%; $p < 0.05$).

The relative density of three fractions was not significantly affected by destabilization of fAβ(1−40) by Myr at pH 7.5, at 37 °C for 6 h (Figure 5F). In the supernatant after centrifugation at 4 °C for 2 h at 16000g, no proteins were detected by the Bradford assay (data not shown). This implies that although Myr could destabilize fAβ(1−40) to visible aggregates (Figure 4E,F), they could not depolymerize fAβ(1−40) to monomers or oligomers of Aβ(1−40).

Characterization of the Novel Fluorescence Emission of Myr Bound to fAβ(1−40). In the presence of fAβ(1−40), Myr gave a novel fluorescence at 575 nm with an excitation maximum at 430 nm (Figure 6A). On the other hand, no significant change in the fluorescence spectra was observed when Myr was mixed with the Aβ(1−40) monomer (Figure 6B). The fluorescence of Myr in the presence of fAβ(1−40) was pH-dependent and exhibited a maximum around pH 7.5 (Figure 6C). On the other hand, the fluorescence of Myr both in the presence and in the absence of the Aβ(1−40) monomer exhibited a similar pH dependency with a maximum around pH 8.5 (Figure 6C). This may clearly indicate that the novel fluorescence emitted at 575 nm with an excitation maximum at 430 nm reflects the specific binding of Myr to fAβ(1−40), possibly the β-sheet structure of them. The fluorescence change was linear from 0 to 50 μM fAβ(1−40) ($R^2 = 0.981$; Figure 6D). Figure 6E shows the fluorescence of increasing concentrations of Myr in the presence of 25 μM fAβ(1−40) at pH 7.5. As the Myr concentration increased, the fluorescence intensity reached a plateau level, indicating that Myr binds to a finite number of specific binding sites on fAβ.

Affinity Analysis of Flavonoids to Aβ/fAβ by SPR. As shown in Figure 7, all compounds examined in this study (Myr, Qur, Mor, Cat, or epi-Cat, 1−25 μM) reacted very weakly with the immobilized Aβ monomer. No increase in the response was observed after addition of freshly prepared flavan-3-ol compounds (Cat and epi-Cat, 1−50 μM) to the immobilized fAβ(1−40) (7700−8060 RU) (Figure 8D,E). In contrast, distinct association and dissociation reactions were observed after addition of freshly prepared flavonol compounds at lower concentrations (0.1−6 μM Myr, 0.1−8 μM Qur, and 1−8 μM Mor) to the immobilized fAβ (Figure 8A−C). When Cat and epi-Cat were preincubated at 37 °C for 30 h, these oxidized compounds reacted weakly and reversibly with the immobilized fAβ(1−40) (data not shown). Since these sensorgrams did not fit well to the Langmuir-type (1:1) binding curves, we did not calculate the association, dissociation, and equilibrium constants. However, these sensorgrams may clearly indicate that most if not all of the

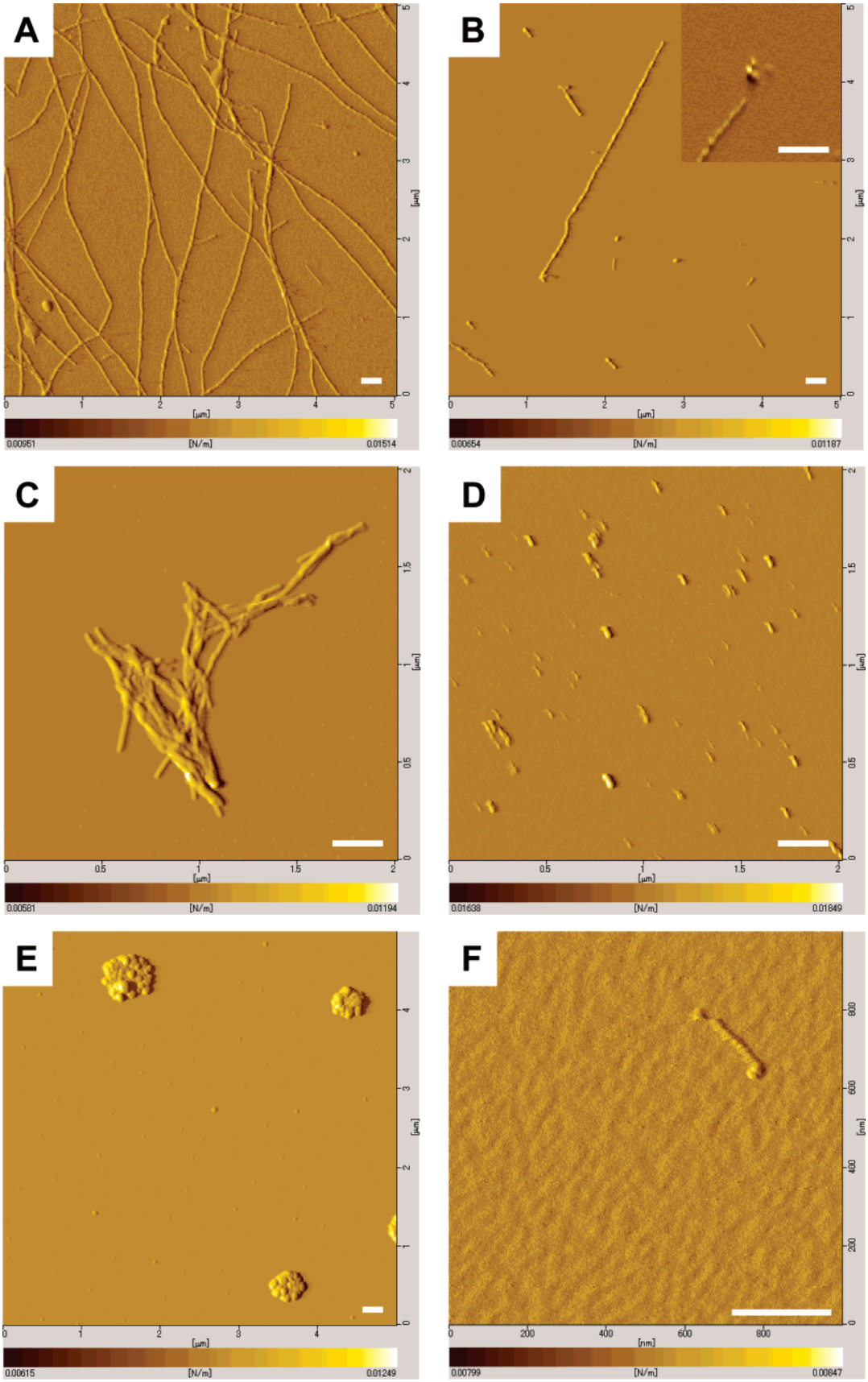

FIGURE 4: Atomic force microscopic assessment of the effects of Myr on formation of fAβ(1−40) from fresh Aβ(1−40) (A and B) and their extension (C and D) and destabilization (E and F). (A and B) The reaction mixture containing 50 μM Aβ(1−40), 50 mM phosphate buffer (pH 7.5), 100 mM NaCl, and 0 (A) or 50 μM Myr (B) was incubated at 37 °C for 7 days. (C and D) The reaction mixture containing 10 μg/mL (2.3 μM) fAβ(1−40), 50 μM Aβ(1−40), 50 mM phosphate buffer (pH 7.5), 100 mM NaCl, and 0 (C) or 50 μM Myr (D) was incubated at 37 °C for 6 h. (E and F) The reaction mixture containing 25 μM fAβ(1−40), 50 mM phosphate buffer (pH 7.5), 100 mM NaCl, and 50 μM Myr was incubated at 37 °C for 6 h. Scale bars indicate a length of 250 nm.

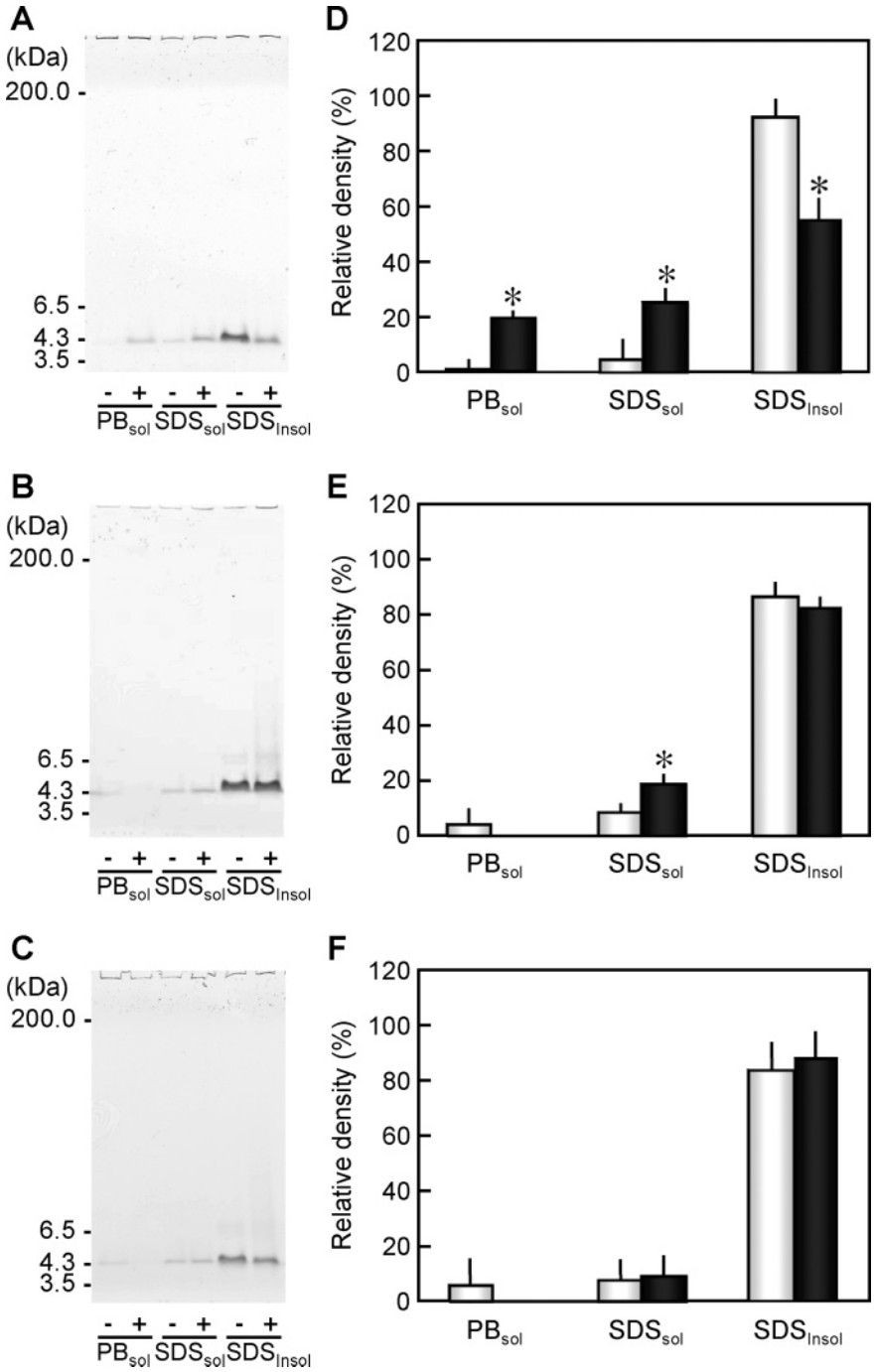

FIGURE 5: Effects of flavonoids on formation of fAβ(1−40) from fresh Aβ(1−40) (A and D) and their extension (B and E) and destabilization (C and F), monitored by SDS−PAGE. (A) The reaction mixture containing 50 μM Aβ(1−40) (lot 550927), 50 mM phosphate buffer (pH 7.5), 100 mM NaCl, and 0 (−) or 50 μM fresh Myr (+) was incubated at 37 °C for 24 h, fractionated into PB_{sol}, SDS_{sol}, and SDS_{Insol} fractions, and then subjected to SDS−PAGE, as described in Experimental Procedures. (B) The reaction mixture containing 10 μg/mL (2.3 μM) fAβ(1−40), 50 μM Aβ(1−40), 50 mM phosphate buffer (pH 7.5), 100 mM NaCl, and 0 (−) or 50 μM fresh Myr (+) was incubated at 37 °C for 6 h and analyzed as described for panel A. (C) The reaction mixture containing 25 μM fAβ(1−40), 50 mM phosphate buffer (pH 7.5), 100 mM NaCl, and 0 (−) or 50 μM fresh Myr (+) was incubated at 37 °C for 6 h and analyzed as described for panel A. (D−F) Semiquantitative densitometric analysis of panels A−C, respectively. Gels in panels A−C were analyzed by densitometry, as described in Experimental Procedures. Both in the absence (gray box) and in the presence of Myr (black box), relative densities of individual fractions are indicated in percent, where the total of PB_{sol}, SDS_{sol}, and SDS_{Insol} fractions is 100%. Boxes and bars denote means ± the standard deviation of four independent experiments. Statistical analysis was conducted with an unpaired *t*-test (asterisks denote a p of <0.05, 0 vs 50 μM fresh Myr in each fraction).

compounds bind reversibly or noncovalently to immobilized fAβ(1−40).

SPR Analysis of the Effect of Myr on the fAβ Extension. Among the flavonoids that were examined, Myr bound most strongly to fAβ and very weakly to monomeric Aβ (Figures 7A and 8A). To evaluate the effect of fibril-bound Myr on the kinetics of fibril extension, we improved the Biacore-based analytical method previously reported by us and another research group (*33*, *38*) (Figure 9A). As shown in Figure 9B, a significant decrease in the rate of extension

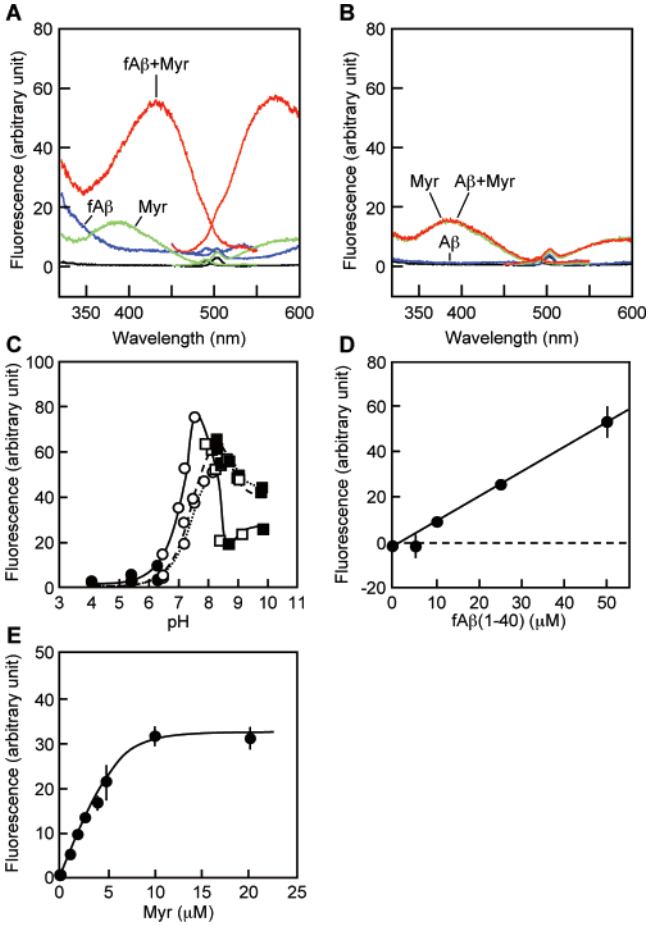

FIGURE 6: Characterization of the novel fluorescence emission of Myr bound to fAβ(1−40). (A) Excitation and emission spectra of fAβ(1−40) with Myr (red), Myr (green), fAβ(1−40) (blue), and a buffer solution (black). The reaction mixture contained 0 or 25 μM fAβ(1−40), 0 or 10 μM Myr, 50 mM phosphate buffer (pH 7.5), and 100 mM NaCl. This is a representative pattern of three independent experiments. (B) Excitation and emission spectra of Aβ(1−40) with Myr (red), Myr (green), Aβ(1−40) (blue), and a buffer solution (black). The reaction mixture contained 0 or 25 μM Aβ(1−40), 0 or 10 μM Myr, 50 mM phosphate buffer (pH 7.5), and 100 mM NaCl. This is a representative pattern of three independent experiments. (C) Effects of pH on the fluorescence of Myr in the absence (•••) or presence of fAβ(1−40) (—) or in the presence of monomeric Aβ(1−40) (- - -). The reaction mixture contained 50 μM Myr, 50 mM buffer, 100 mM NaCl, and 0 (•••) or 25 μM fAβ(1−40) (—), or 25 μM monomeric Aβ(1−40) (- - -). The buffers used were citrate buffer at pH 4−6 (●), phosphate buffer at pH 6−8 (○), Tris-HCl buffer at pH 8−9 (□), and glycine-NaOH buffer at pH 8.5−10 (■). Each point represents the mean of triplicate determinations. This is a representative pattern of three independent experiments. (D) Effect of fAβ(1−40) concentration on the fluorescence. The reaction mixture contained 50 μM Myr, 50 mM phosphate buffer (pH 7.5), 100 mM NaCl, and indicated concentrations of fAβ(1−40). Each point represents the mean ± the standard deviation of triplicate determinations. A linear least-squares fit was performed for a straight line ($R^2 = 0.981$). (E) Effect of Myr concentration on the fluorescence. The reaction mixtures contained 25 μM fAβ(1−40), 50 mM phosphate buffer (pH 7.5), 100 mM NaCl, and the indicated concentrations of Myr. Each point represents the mean ± the standard deviation of triplicate determinations.

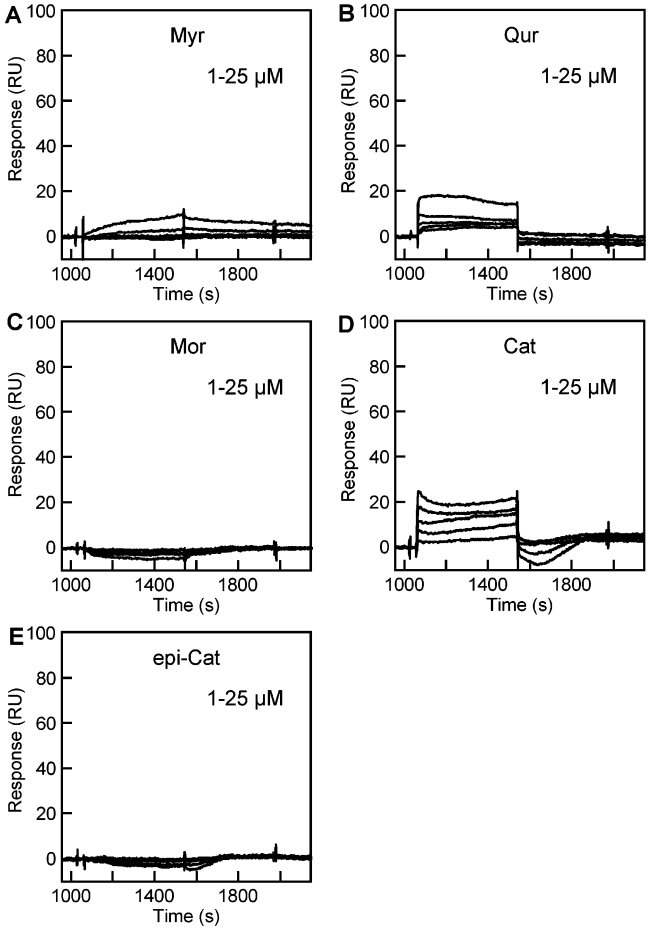

FIGURE 7: Analysis of the affinity of flavonoids for the Aβ monomer by SPR. Flavonoids [Myr (A), Qur (B), Mor (C), Cat (D), and epi-Cat (E), 0, 1, 3, 6, 12, and 25 μM, 240 μL] dissolved in the running buffer [50 mM phosphate (pH 7.5), 100 mM NaCl, 3 mM EDTA, 0.005% Tween 20, and 1% DMSO] were injected over the reference and Cys-Aβ(1−40)- (3800−4300 RU) or Aβ-(1−40)-immobilized (for Mor only, 700 RU) flow cells. The obtained sensorgrams were compensated using double referencing, and solvent effects were further compensated by the DMSO calibration procedure as described in Experimental Procedures.

was observed when >0.5 μM Myr was injected. The maximum inhibition (approximately 30%) was achieved by the injection of >5 μM Myr. A reasonable interpretation of these data could be that the binding of Myr to the fibrils, particularly to their growing ends, may compete with the binding of the Aβ monomer to fibril ends and inhibit subsequent polymeriztion of Aβ into fibrils, resulting in the inhibition of fibril extension (Figure 9A).

DISCUSSION

These findings showed that flavonoids, especially Myr, exert anti-amyloidogenic effects on fAβ predominantly by binding preferentially and reversibly to the amyloid fibril structure of fAβ, rather than to the certain primary structure of Aβ monomers.

Several key pieces of evidence support this conclusion. First, MALDI-TOF mass spectrometry analyses of Aβ isolated from Myr-destabilized fAβ did not reveal any Myr−Aβ adducts or dehydrated, oxidized, or oligomerized Aβ (data not shown). The lack of Myr−Aβ adducts suggests that Myr may bind reversibly or noncovalently to Aβ in fAβ. Moreover, these findings imply that this inhibition should be effective at substoichiometric concentrations of Myr. Actually, the effective concentrations (EC_{50}) of Myr for the formation of fAβ(1−40) from 50 μM Aβ(1−40), fibril

extension with 50 μM Aβ(1−40), and destabilization of 25 μM fAβ(1−40) were 0.29, 0.22, and 1.8 μM, respectively (*13*). Second, only in the presence of fAβ(1−40) at pH 7.5 did Myr represent a novel fluorescence at 575 nm with an excitation maximum at 430 nm (Figure 6A−C). Krebs et al. reported that the dipole excitation axis of ThT lies parallel to the long molecular axis of amyloid fibrils, using confocal microscopy with polarized laser light (*39*). They proposed that binding of ThT occurs in "channels" that run along the length of the β-sheet. Thus, it may be reasonable to consider that the novel fluorescence emitted at 575 nm with an excitation maximum at 430 nm reflects the specific binding of Myr possibly to the cross-β structure of fAβ(1−40). Dangles et al. reported that Qur displays a very strong fluorescence emission band around 530 nm (excitation at 450 nm) when dissolved in a pH 7.4 phosphate buffer containing bovine serum albumin (BSA) (*40*). They suggested that some highly fluorescent pyrylium tautomers could be specifically stabilized upon noncovalent binding to BSA. These data also suggest that when administered to humans, Myr may be carried by binding to human serum albumin and its activity may be regulated by the equilibrium between free and albumin-bound forms. Finally, SPR analysis represented distinct association and dissociation reactions of flavonols (Myr, Qur, and Mor) with fAβ(1−40), in contrast to the very weak binding to the Aβ monomer (Figures 7 and 8). These data may indicate that most if not all of the compounds bind reversibly or noncovalently to immobilized fAβ(1−40). The high-affinity binding of flavonols to fAβ-(1−40) relative to the low-affinity binding of flavan-3-ols (Cat and epi-Cat) (Figure 8) correlates well with the effective concentrations of polyphenols for the formation, extension, and destabilization of fAβ(1−40) (*13*). Additionally, the high-affinity binding of Myr to fAβ(1−40) may be associated with the formation of a stable autoxidative intermediate as indicated by the rapid increase in the magnitude of the peak at around 320−327 nm (Figure 2A). Interestingly, using gel filtration, ultracentrifugation, and spectrophotometry, Taniguchi et al. reported that Myr, a potent polyphenol inhibitor of tau filament formation, binds more strongly to filamentous and aged soluble tau than to the monomeric protein, suggesting the preferential binding of Myr to tau in a cross-β conformation (*27*).

Several research groups have proposed that the covalent modification of amyloidogenic proteins by certain organic compounds resulting in the stabilization of protein oligomers may be the potential mechanism for the inhibition of amyloid fibril formation by these organic compounds. First, Conway et al. showed that dopamine or L-dopa inhibits the fibrillization of recombinant α-synuclein (α-syn) filaments, presumably through formation of a covalent adduct of the orthoquinone derivative of dopamine with α-syn and stabilization of α-syn into "protofibrillar" structures that are incompetent in forming fibrils (*41*). Second, Zhu et al. reported that the flavonoid baicalein, and especially its oxidized forms, inhibit fibrillation of α-syn and disaggregate existing fibrils (*42*). They observed that the product of the inhibition reaction is predominantly a soluble oligomer of α-syn, in which the protein molecules have been covalently modified by baicalein quinone to form a Schiff base with a lysine side chain in α-syn. Third, Li et al. showed that dopamine, L-dopa, and especially its oxidized forms inhibit

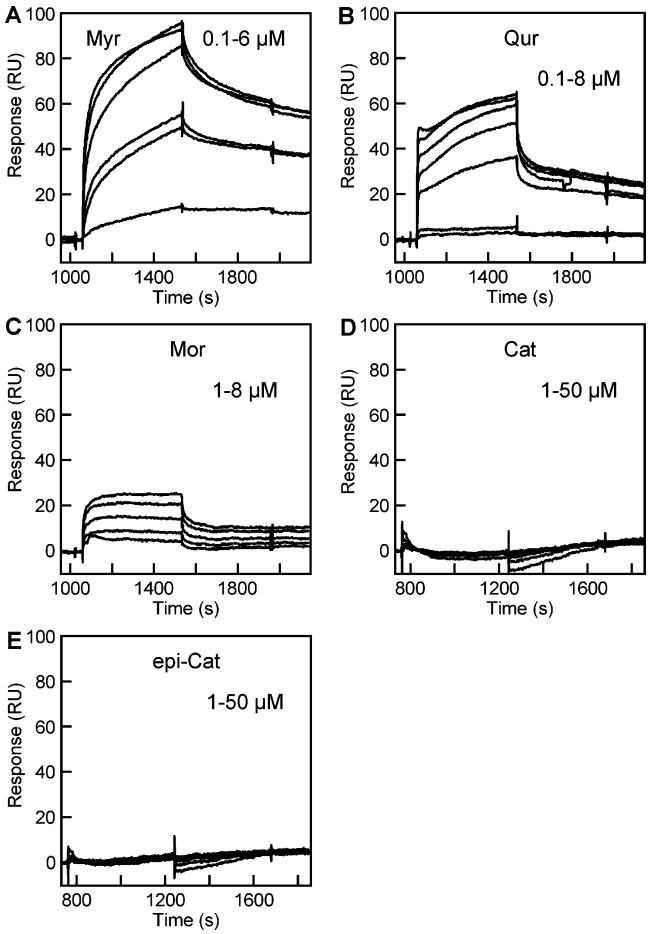

FIGURE 8: Analysis of the affinity of flavonoids for fAβ by SPR. Myr [(A) 0, 0.1, 0.5, 1, 2, 4, and 6 μM], Qur [(B) 0, 0.1, 0.5, 1, 2, 4, 6, and 8 μM], Mor [(C) 0, 1, 2, 4, 6, and 8 μM], Cat [(D) 0, 1, 3, 6, 12, 25, and 50 μM], and epi-Cat [(E) 0, 1, 3, 6, 12, 25, and 50 μM] solutions were injected over the reference and fAβ-immobilized (7700−8060 RU) flow cells, and data were processed as described in the legend of Figure 7.

fibrillation of α-syn and Aβ and disaggregate existing fibrils (*43*). They indicated that the product of the inhibition reaction is predominantly a stable oligomer of α-syn, in which the protein molecules have been covalently modified by catecholamine quinones to form a Schiff base with a lysine side chain in α-syn. Finally, Taniguchi et al. reported the formation of soluble oligomeric tau in the presence of phenothiazines, polyphenols, and porphyrins (*27*). They suggested that these compounds may be inhibitory toward heparin-induced tau filament assembly by virtue of their ability to bind covalently to and stabilize disulfide-linked oligomeric tau, an intermediate in the pathway from monomeric to filamentous tau. At present, we cannot rule out completely the possibility that a small amount of Myr−Aβ adducts could be formed and inhibit fAβ formation by stabilizing protein oligomers. On the other hand, consistent with our working model, Norris et al. have recently observed that dopamine reversibly inhibits α-syn fibrillization by acting as a molecular chaperone and inducing conformational changes in α-syn that can occur through the interaction of dopaminochrome with the ^{125}YEMPS^{129} motif of α-syn (*44*). Further experiments are essential for determining whether certain organic compounds, such as Myr, could covalently modify Aβ to exert anti-amyloidogenic effects in vitro.

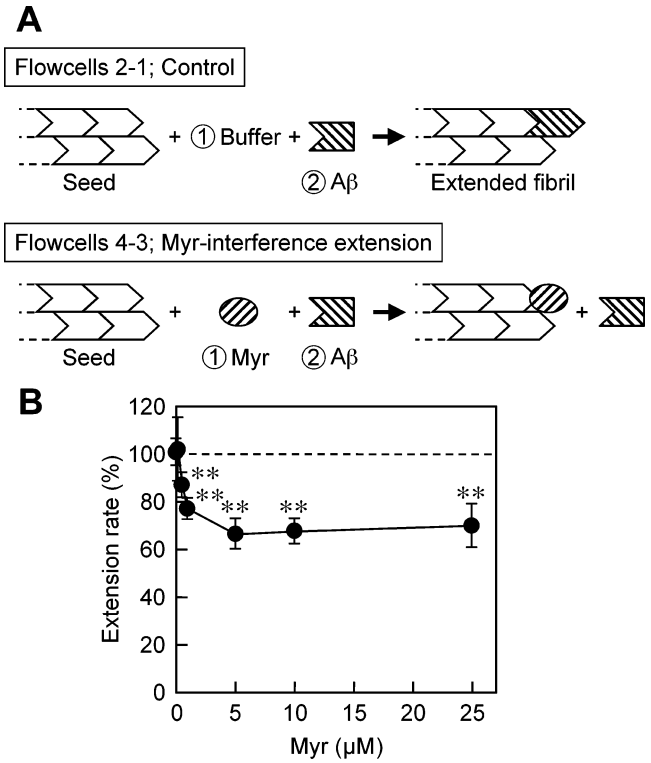

FIGURE 9: SPR analysis of the effect of Myr on fAβ extension. (A) Reaction scheme of extension with or without Myr. The seed fAβ was immobilized onto the surface of flow cells 2 and 4 (512−600 RU). Blank cells 1 and 3 were prepared as described in Experimental Procedures. For the positive control reaction, 100 μL of running buffer was injected into flow cells 2 and 1, followed by the injection of a 5 μM Aβ solution (30 μL) using COINJECT mode. The effect of Myr on the reaction was examined by injecting 100 μL of a Myr solution (0, 0.2, 0.5, 1, 2, 5, 10, or 25 μM) into flow cells 4 and 3, followed by the injection of an Aβ solution. The rate of the extension reaction was calculated from the increase in the magnitude of the SPR response signal during the addition of Aβ solution. The ratio of inhibition was calculated by dividing the rate of extension with Myr by the rate of positive control at the same cycle. (B) Concentration-dependent inhibitory effect of Myr on the extension rate of fAβ. Points and bars represent the average and standard deviation of four experiments, respectively. Asterisks denote a p of <0.01 (one-way analysis of variance with the post-hoc test by Dunnett).

Oxidized Qur inhibited fAβ(1−40) formation significantly more potently than fresh Qur (Figure 3A), and oxidized Myr, Mor, Cat, and epi-Cat inhibited fAβ(1−40) extension significantly more potently than fresh compounds (Figure 3B). Many research groups also have reported that oxidized forms of various organic compounds exhibit more potent anti-amyloidogenic activities than their fresh forms (*39*, *41*−*43*). As shown in Figure 9, oxidized flavonoids may bind to the growing ends of fibrils with a higher affinity than fresh forms, resulting in the inhibition of polymerization of Aβ monomers onto the fibril ends. On the other hand, fresh Qur and Mor destabilized fAβ(1−40) significantly more potently than oxidized compounds (Figure 3C). While we have no clear explanation for this finding, the mechanism of destabilizing fAβ(1−40) may be different from that of inhibiting fAβ(1−40) formation and extension. Destabilization of fibrils could involve preferential noncovalent interactions of the fresh flavonoids with the fibrils themselves, leading to weakening of the intermolecular forces in the fibrils and resulting in their destabilization. Further studies are essential to revealing the molecular mechanism of fibril destabilization by organic compounds.

In conclusion, we demonstrated that flavonoids especially Myr exert an anti-amyloidogenic effect in vitro by preferentially and reversibly binding to the amyloid fibril structure of fAβ, rather than to Aβ monomers. Although further experiments are essential to reveal the anti-amyloidogenic mechanisms of various organic compounds, this working model should prove useful for the rational development of preventives and therapeutics for AD and other human amyloidoses.

ACKNOWLEDGMENT

We are grateful to H. Okada and N. Takimoto for excellent technical assistance.

REFERENCES

1. Selkoe, D. J. (2001) Alzheimer's disease: Genes, proteins, and therapy, *Physiol. Rev. 81*, 741−766.
2. Hardy, J., and Selkoe, D. J. (2002) The amyloid hypothesis of Alzheimer's disease: Progress and problems on the road to therapeutics, *Science 297*, 353−356.
3. Doody, R. S., Stevens, J. C., Beck, C., Dubinsky, R. M., Kaye, J. A., Gwyther, L., Mohs, R. C., Thal, L. J., Whitehouse, P. J., DeKosky, S. T., and Cummings, J. L. (2001) Practice parameter: Management of dementia (an evidence-based review). Report of the Quality Standards Subcommittee of the American Academy of Neurology, *Neurology 56*, 1154−1166.
4. Schenk, D., Barbour, R., Dunn, W., Gordon, G., Grajeda, H., Guido, T., Hu, K., Huang, J., Johnson-Wood, K., Khan, K., Kholodenko, D., Lee, M., Liao, Z., Lieberburg, I., Motter, R., Mutter, L., Soriano, F., Shopp, G., Vasquez, N., Vandevert, C., Walker, S., Wogulis, M., Yednock, T., Games, D., and Seubert, P. (1999) Immunization with amyloid-β attenuates Alzheimer-disease-like pathology in the PDAPP mouse, *Nature 400*, 173−177.
5. Cherny, R. A., Atwood, C. S., Xilinas, M. E., Gray, D. N., Jones, W. D., McLean, C. A., Barnham, K. J., Volitakis, I., Fraser, F. W., Kim, Y.-S., Huang, X., Goldstein, L. E., Moir, R. D., Lim, J. T., Beyreuther, K., Zheng, H., Tanzi, R. E., Masters, C. L., and Bush, A. I. (2001) Treatment with a copper-zinc chelator markedly and rapidly inhibits β-amyloid accumulation in Alzheimer's disease transgenic mice, *Neuron 30*, 665−676.
6. Jarrett, J. T., and Lansbury, P. T., Jr. (1993) Seeding "one-dimensional crystallization" of amyloid: A pathogenic mechanism in Alzheimer's disease and scrapie? *Cell 73*, 1055−1058.
7. Lomakin, A., Teplow, D. B., Kirschner, D. A., and Benedek, G. B. (1997) Kinetic theory of fibrillogenesis of amyloid β-protein, *Proc. Natl. Acad. Sci. U.S.A. 94*, 7942−7947.
8. Naiki, H., Gejyo, F., and Nakakuki, K. (1997) Concentration-dependent inhibitory effects of apolipoprotein E on Alzheimer's β-amyloid fibril formation in vitro, *Biochemistry 36*, 6243−6250.
9. Naiki, H., and Gejyo, F. (1999) Kinetic analysis of amyloid fibril formation, *Methods Enzymol. 309*, 305−318.
10. Naiki, H., Hasegawa, K., Yamaguchi, I., Nakamura, H., Gejyo, F., and Nakakuki, K. (1998) Apolipoprotein E and antioxidants have different mechanisms of inhibiting Alzheimer's β-amyloid fibril formation in vitro, *Biochemistry 37*, 17882−17889.
11. Ono, K., Hasegawa, K., Yoshiike, Y., Takashima, A., Yamada, M., and Naiki, H. (2002) Nordihydroguaiaretic acid potently breaks down pre-formed Alzheimer's β-amyloid fibrils in vitro, *J. Neurochem. 81*, 434−440.
12. Ono, K., Hasegawa, K., Naiki, H., and Yamada, M. (2004) Curcumin has potent anti-amyloidogenic effects for Alzheimer's β-amyloid fibrils in vitro, *J. Neurosci. Res. 75*, 742−750.
13. Ono, K., Yoshiike, Y., Takashima, A., Hasegawa, K., Naiki, H., and Yamada, M. (2003) Potent anti-amyloidogenic and fibril-destabilizing effects of polyphenols in vitro: Implications for the prevention and therapeutics of Alzheimer's disease, *J. Neurochem. 87*, 172−181.
14. Ono, K., Hasegawa, K., Naiki, H., and Yamada, M. (2004) Anti-amyloidogenic activity of tannic acid and its activity to destabilize

Alzheimer's β-amyloid fibrils in vitro, *Biochim. Biophys. Acta 1690*, 193−202.
15. Ono, K., Yoshiike, Y., Takashima, A., Hasegawa, K., Naiki, H., and Yamada, M. (2004) Vitamin A exhibits potent antiamyloidogenic and fibril-destabilizing effects in vitro, *Exp. Neurol. 189*, 380−392.
16. Ono, K., Hasegawa, K., Yamada, M., and Naiki, H. (2002) Nicotine breaks down preformed Alzheimer's β-amyloid fibrils in vitro, *Biol. Psychiatry 52*, 880−886.
17. Ono, K., Hasegawa, K., Naiki, H., and Yamada, M. (2005) Preformed β-amyloid fibrils are destabilized by coenzyme Q10 in vitro, *Biochem. Biophys. Res. Commun. 330*, 111−116.
18. Hirohata, M., Ono, K., Naiki, H., and Yamada, M. (2005) Nonsteroidal anti-inflammatory drugs have anti-amyloidogenic effects for Alzheimer's β-myloid fibrils in vitro, *Neuropharmacology 49*, 1088−1099.
19. Ono, K., Hasegawa, K., Naiki, H., and Yamada, M. (2006) Anti-Parkinsonian agents have anti-amyloidogenic activity for Alzheimer's β-amyloid fibrils in vitro, *Neurochem. Int. 48*, 275−285.
20. Tomiyama, T., Asano, S., Suwa, Y., Morita, T., Kataoka, K., Mori, H., and Endo, N. (1994) Rifampicin prevents the aggregation and neurotoxicity of amyloid β protein in vitro, *Biochem. Biophys. Res. Commun. 204*, 76−83.
21. Tomiyama, T., Shoji, A., Kataoka, K., Suwa, Y., Asano, S., Kaneko, H., and Endo, N. (1996) Inhibition of amyloid β protein aggregation and neurotoxicity by rifampicin. Its possible function as a hydroxyl radical scavenger, *J. Biol. Chem. 271*, 6839−6844.
22. Kisilevsky, R., Lemieux, L. J., Fraser, P. E., Kong, X., Hultin, P. G., and Szarek, W. A. (1995) Arresting amyloidosis in vivo using small-molecule anionic sulphonates or sulphates: Implications for Alzheimer's disease, *Nat. Med. 1*, 143−148.
23. Soto, C., Kindy, M. S., Baumann, M., and Frangione, B. (1996) Inhibition of Alzheimer's amyloidosis by peptides that prevent β-sheet conformation, *Biochem. Biophys. Res. Commun. 226*, 672−680.
24. Pappolla, M., Bozner, P., Soto, C., Shao, H., Robakis, N. K., Zagorski, M., Frangione, B., and Ghiso, J. (1998) Inhibition of Alzheimer β-fibrillogenesis by melatonin, *J. Biol. Chem. 273*, 7185−7188.
25. Forloni, G., Colombo, L., Girola, L., Tagliavini, F., and Salmona, M. (2001) Anti-amyloidogenic activity of tetracyclines: Studies in vitro, *FEBS Lett. 487*, 404−407.
26. Zeng, H., Zhang, Y., Peng, L., Shao, H., Menon, N. K., Yang, J., Salomon, A. R., Freidland, R. P., and Zagorski, M. G. (2001) Nicotine and amyloid formation, *Biol. Psychiatry 49*, 248−257.
27. Taniguchi, S., Suzuki, N., Masuda, M., Hisanaga, S., Iwatsubo, T., Goedert, M., and Hasegawa, M. (2005) Inhibition of heparin-induced tau filament formation by phenothiazines, polyphenols, and porphyrins, *J. Biol. Chem. 280*, 7614−7623.
28. Bradford, M. M. (1976) A rapid and sensitive method for the quantitation of microgram quantities of protein utilizing the principle of protein-dye binding, *Anal. Biochem. 72*, 248−254.
29. Hasegawa, K., Yamaguchi, I., Omata, S., Gejyo, F., and Naiki, H. (1999) Interaction between Aβ(1−42) and Aβ(1−40) in Alzheimer's β-amyloid fibril formation in vitro, *Biochemistry 38*, 15514−15521.
30. Naiki, H., and Nakakuki, K. (1996) First-order kinetic model of Alzheimer's β-amyloid fibril extension in vitro, *Lab. Invest. 74*, 374−383.
31. Schägger, H., and von Jagow, G. (1987) Tricine-sodium dodecyl sulfate-polyacrylamide gel electrophoresis for the separation of proteins in the range from 1 to 100 kDa, *Anal. Biochem. 166*, 368−379.
32. Cairo, C. W., Strzelec, A., Murphy, R. M., and Kiessling, L. L. (2002) Affinity-based inhibition of β-amyloid toxicity, *Biochemistry 41*, 8620−8629.
33. Hasegawa, K., Ono, K., Yamada, M., and Naiki, H. (2002) Kinetic modeling and determination of reaction constants of Alzheimer's β-amyloid fibril extension and dissociation using surface plasmon resonance, *Biochemistry 41*, 13489−13498.
34. Frostell-Karlsson, Å., Remaeus, A., Roos, H., Andersson, K., Borg, P., Hämäläinen, M., and Karlsson, R. (2000) Biosensor analysis of the interaction between immobilized human serum albumin and drug compounds for prediction of human serum albumin binding levels, *J. Med. Chem. 43*, 1986−1992.
35. Mabry, T. J., Markham, K. R., and Thomas, M. B. (1970) *The systematic identification of flavonoids*, Springer-Verlag, Berlin.
36. Dangles, O., Fargeix, G., and Dufour, C. (1999) One-electron oxidation of quercetin and quercetin-derivatives in protic and non protic media, *J. Chem. Soc., Perkin Trans. 2*, 1387−1395.
37. Lazarus, S. A., Hammerstone, J. F., Adamson, G. E., and Schmitz, H. H. (2001) High-performance liquid chromatography/mass spectrometry analysis of proanthocyanidins in food and beverages, *Methods Enzymol. 335*, 46−57.
38. Kakuyama, H., Söderberg, L., Horigome, K., Winblad, B., Dahlqvist, C., Näslund, J., and Tjernberg, L. O. (2005) CLAC binds to aggregated Aβ and Aβ fragments, and attenuates fibril elongation, *Biochemistry 44*, 15602−15609.
39. Krebs, M. R., Bromley, E. H., and Donald, A. M. (2005) The binding of thioflavin-T to amyloid fibrils: Localisation and implications, *J. Struct. Biol. 149*, 30−37.
40. Dangles, O., Dufour, C., Manach, C., Morand, C., and Remesy, C. (2001) Binding of flavonoids to plasma proteins, *Methods Enzymol. 335*, 319−333.
41. Conway, K. A., Rochet, J. C., Bieganski, R. M., and Lansbury, P. T., Jr. (2001) Kinetic stabilization of the α-synuclein protofibril by a dopamine-α-synuclein adduct, *Science 294*, 1346−1349.
42. Zhu, M., Rajamani, S., Kaylor, J., Han, S., Zhou, F., and Fink, A. L. (2004) The flavonoid baicalein inhibits fibrillation of α-synuclein and disaggregates existing fibrils, *J. Biol. Chem. 279*, 26846−26857.
43. Li, J., Zhu, M., Manning-Bog, A. B., Di Monte, D. A., and Fink, A. L. (2004) Dopamine and L-dopa disaggregate amyloid fibrils: Implications for Parkinson's and Alzheimer's disease, *FASEB J. 18*, 962−964.
44. Norris, E. H., Giasson, B. I., Hodara, R., Xu, S., Trojanowski, J. Q., Ischiropoulos, H., and Lee, V. M. (2005) Reversible inhibition of α-synuclein fibrillization by dopaminochrome-mediated conformational alterations, *J. Biol. Chem. 280*, 21212−21219.

BI061540X